Netsu Sokutei **32** (2) 70-76

解　説

High Sensitive Differential AC-Chip Calorimeter for Nanogram Samples#

Heiko Huth, Alexander Minakov, and Christoph Schick

(Received February 4, 2005; Accepted February 9, 2005)

A differential AC chip calorimeter based on commercially available sensors is described. Due to the differential setup pJK^{-1} sensitivity is achieved. Heat capacity can be measured for sample masses below one nanogram. This corresponds to heat capacities below one nJK^{-1} even above room temperature as needed for the study of the glass transition in nanometer thin polymeric films. The calorimeter allows for the frequency dependent measurement of complex heat capacity in the broad frequency range from 1 Hz to 1 kHz for sample masses of some nanograms.

Introduction

Calorimetry is known as a very powerful tool for the characterization of a wide variety of materials and their transitions. There is an ongoing interest in improving the technique in order to achieve high sensitivity and precision. High sensitive differential scanning calorimeters are developed mainly to measure biological samples showing small effects in highly diluted systems, *e.g.*[1,2] For reduced sample masses AC-calorimetric techniques are used in this field too.[3] For more than 30 years, AC-calorimetry has been known as a sensitive technique to measure thermophysical properties of small sized samples. Based on the pioneering works of Corbino,[4] Kraftmakher[5] and Sullivan and Seidel[6] a large variety of different designs was used for AC-calorimetry. For the review, see.[7] To further increase sensitivity a differential AC-calorimeter was developed too.[8]

In order to allow measurements on sub micron films addenda heat capacity has to be reduced dramatically. The combination of silicon technology and calorimetry opens up new possibilities in this research area as demonstrated recently.[9,10] The thin membrane gives the possibility to decrease the size of the measured sample. They offer a good ratio between sample and addenda heat capacity for sub micron films. While most of the chip calorimeters are used for samples in the microgram range[11,12] specialized home made sensors are used to measure nanogram samples.[13,14] Magnetic effects in nanometer sized films, for example, are observed using chip calorimeter in relaxation mode at low temperatures.[9,15] Using chip calorimeter in high vacuum under essentially adiabatic conditions the glass transition in polymer films down to 3 nm is measured.[13] This is realized using a fast scanning calorimeter at heating rates up to 1,000,000 $K\,s^{-1}$.[14] Also differential setups are possible with this technique.[16] Because of the essentially adiabatic conditions only measurements at rapid heating are possible.[17]

Thin film calorimeter operating under non-adiabatic conditions allow heating as well as cooling at rates up to 10,000 $K\,s^{-1}$ [18,19,20] and possibly faster.[21] Using such high rates yields often non-equilibrium states of the sample under investigation. As an example, for several fast crystallizing polymers it is possible to prevent crystallization on cooling totally and to reach the amorphous glassy state.[18,19] Another example is the superheating of polymer crystals at fast heating.[22-24] But often one would prefer to measure thermal properties of small samples at or at least close to thermodynamic

Presented in part at the 40th Japanese Conference on Calorimetry and Thermal Analysis, Tokyo, October 12 to 14, 2004.

equilibrium. This can be achieved by a combination of chip calorimetry and AC calorimetry.[9] As common in AC calorimetry a small periodic heat flow is provided and the resulting complex temperature amplitude is measured. The measurements are done at slow scanning or at constant bath temperature. The frequency chosen provides a well defined time scale of the experiment. In several cases, *e.g.* at glass transition, a direct comparison with results from other dynamic methods like dielectric spectroscopy is possible.[25] Such an AC-chip calorimeter for small samples using a single commercially available sensor under non-adiabatic conditions is described in.[26] The sensitivity of this system is about 10 nJ K^{-1} at room temperature. This setup would allow measuring the glass transition of polymer films down to 500 nm thickness. For measuring the glass transition of much thinner polymer films the sensitivity of the calorimeter has to be enhanced.

Based on a differential AC-calorimeter we show an improved experimental setup combining the advantages of the different methods already described. The differential AC chip calorimeter is based on a commercially available chip sensor,[11] which was already used in[19,26,27] for AC and in[18,19,22-24] for fast scanning calorimetry. Due to the differential setup we achieve a sensitive in the pico Joule per Kelvin range allowing to measure samples below one nanogram. Consequently films down to 1 nm thickness can be measured. Because of the small total heat capacity (addenda + sample) not only a high sensitivity is achieved but AC measurements at relative high frequencies are possible too.[27] The calorimeter allows heat capacity measurements in the frequency range 1 Hz to 1 kHz.

Experimental

The described differential AC calorimetric method is based on the thermal behavior of a single sensor under non-adiabatic conditions, which is described in detail in.[26] Therefore we start with a brief description of the thermal behavior of the sensor before going into details of the differential setup.

In AC calorimetry the apparent heat capacity is given by

$$C_{ap}(\omega) = P_0 \,/\, i\omega T_A \qquad (1)$$

with P_0 the amplitude of the applied power at the frequency ω and T_A the complex amplitude of the temperature modulation. Let us consider a chip calorimeter based on a thin membrane operated in a gas surrounding. If the membrane is thin enough, the heat transfer through the gas is dominant. The lateral heat transfer through the membrane can be neglected in a first approximation model.[18] Then, the heat transfer through the gas from the small central heated region of the membrane can be estimated as follows. The heater is considered as a point source of the heat transferred in the gas.[18,26] In this case the temperature in the gas near the heater is described by the spherical wave $T_g(t,r) \propto \exp(i\omega t - k_g r)/r$, where $k^2_g = i\omega \rho_g c_g / \lambda_g$ with λ_g thermal conductivity, c_g specific heat capacity and ρ_g density of the surrounding gas. The heat loss through the gas can be described by the heat exchange coefficient $G = 4\pi r_0 \lambda_g$ with the radius of the heated area r_0, which is small compared to the dimension of the membrane in lateral direction and the distance from the heater to the nearest boundary. The parameter G can be estimated as *ca.* $2 \cdot 10^{-5}$ W K^{-1} in air atmosphere at room temperature and pressures in the range $10^3 \sim 10^5$ Pa with $\lambda_g = 0.026$ W K^{-1} m^{-1} and $r_0 = 50$ μm. The estimation is in good agreement with the experiment. The parameter G can be considered as frequency independent in the range 1 ~ 1000 Hz with good accuracy.[26] Solving the Fourier heat flux equation for such a system one gets for the temperature-modulation amplitude of the heated membrane area:

$$T_A(\omega) = P_0 \,/\, (i\omega C + G) \qquad (2)$$

Where C is the total heat capacity of the sample with the addenda. From Eq.1 and Eq.2 one can find $C_{ap}(\omega) = C + G / i\omega$. The term $G / i\omega$ in the apparent heat capacity describes the heat loss through the surrounding gas. The further contributions to the apparent heat capacity are determined as follows. The effective heat capacity of the sample with a finite sample thickness d_S is given by $C_S \cdot \tanh(\alpha_S)/\alpha_S$, where the effective thermal thickness α_S of the sample is defined as the thickness d_S times thermal-wave number $\alpha_S = d_S \cdot k_S$ ($k^2 = i\omega\rho c/\lambda$ for a substance with corresponding parameters λ, c and ρ). For thin films $|\alpha_S| \ll 1$ and then the factor $\tanh(\alpha_S)/\alpha_S$ equals one with high precision up to 10 kHz. The size of the heated area of the sensor is frequency dependent and becomes smaller with higher frequencies. Thus the apparent addenda heat capacity can be approximated as

$C_0(\omega)=C_{00}\cdot(1+(\omega_0/i\omega)^{1/2})$.[26] Another influence is the difference between measured temperature and the actual temperature of the sample because of the distance between heater and thermopile, which gives a factor $\cosh(\alpha_0)$.[28] In this case the effective thermal thickness $\alpha_0=k_0\cdot d_0$ is applied for the distance between heater and thermopile d_0. Considering all these contributions one gets for the apparent heat capacity in Eq.1:

$$C_{ap}(\omega)=\cosh(\alpha_0)\cdot\{C_0(\omega)+C_S\cdot\tanh(\alpha_S)/\alpha_S+G/i\omega\} \quad (3)$$

The parameters $\alpha=\alpha_0(i\omega)^{1/2}$, ω_0, and C_{00} are determined from the frequency dependence of the signal for the empty sensor. The sensitivity of the thermopile and the heat exchange coefficient G are obtained simultaneously for any fixed temperature from the frequency dependence measured in the range say from 0.1 Hz to 1 kHz as in.[26]

This approach was successfully applied to the determination of the heat capacity of a 3.8 μg sample of Ruthenium doped $CeFe_2$ and its magnetic phase transitions under the influence of strong magnetic fields.[26] The aim of the present study is the thermal characterization of nm thick films. For such thin films the sample heat capacity C_S is much smaller than C_0 and consequently the first term in Eq.3 dominates the apparent heat capacity. One possibility to minimize the influence of the addenda heat capacity is the usage of a differential setup. The basic equations for such a differential setup will be discussed next.

For the difference of the thermopile signal amplitudes $\Delta T_A=T_{A0}-T_{AS}$ of an empty sensor T_{A0} and a sensor with a sample T_{AS} the following equation holds:

$$\frac{i\omega\cosh(\alpha_0)\Delta T_A}{P_0} = \frac{1}{C_0(\omega)+G/i\omega}-\frac{1}{C_0(\omega)+C_S+G/i\omega}\cong\frac{C_S}{(C_0(\omega)+G/i\omega)^2} \quad (4)$$

where the term C_S was neglected with respect to C_0 assuming $C_S\ll C_{00}$. With an effective heat capacity of the empty cell $\widetilde{C}=C_0(\omega)+G/i\omega$ one gets $i\omega\cosh(\alpha_0)\Delta T_A/P_0=C_S/\widetilde{C}^2$. In this formula two identical sensors are assumed.

The differences of the sensors can be taken into account measuring the empty differential system. In this case Eq.4 is extended assuming a small difference in C_0 and G between the two sensors. With $C_0'=C_0+\delta C_0$ and $G'=G+\delta G$ for one of the sensors Eq.4 gives for the empty differential system

$$\frac{i\omega\cosh(\alpha_0)\Delta T_{A0}}{P_0}=\frac{\delta C_0+\delta G/i\omega}{(C_0+/i\omega)_2} \quad (5)$$

and for the differential system loaded with a sample

$$\frac{i\omega\cosh(\alpha_0)\Delta T_{AS}}{P_0}=\frac{C_S+\delta C_0+\delta G/i\omega}{(C_0+/i\omega)_2} \quad (6)$$

The temperature amplitude is given by the voltage amplitude U at the thermopile divided by the thermopile sensitivity S. For the case of two empty sensors the differential thermopile signal is denoted by ΔU_0 and for the case with the sample by ΔU. In terms of the measured quantities the heat capacity of the sample for the non-ideally symmetric system is then given by

$$C_S=\frac{i\omega\cosh(\alpha_0)\widetilde{C}^2}{SP_0}\ [\Delta U-\Delta U_0] \quad (7)$$

Eq.7 is valid for thin (submicron) samples. If the sample thickness increases, the factor $\tanh(\alpha_S)/\alpha_S$ has to be taken into account.

The above considerations were taken into account for a differential AC chip calorimeter based on a commercially available pressure gauge from Xensor Integrations, NL,[11] see **Fig.1**. In the centre of a free standing 500 nm thin silicon-nitride membrane a small heater is placed. The heater consists of two parallel

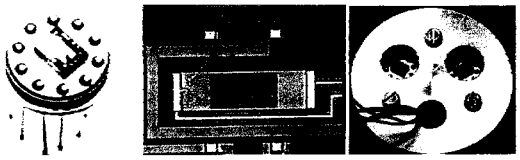

Fig.1 Chip sensor for the AC calorimeter. The left hand picture shows the thermal conductive vacuum gauge from Xensor integrations NL. The middle picture shows the magnified center area of the membrane with the heater indicated by the arrow and four hot junctions of the thermopile (bright squares). The right hand picture shows the chip sensors mounted in the differential setup. The diameter of the aluminum block is 36 mm and mounted in the cryostat.

stripes of 50 µm distance. The temperature distribution in the area between the stripes is almost uniform as shown in.[20] Around the heater the six hot junctions of a thermopile are arranged. The heater, thermopile, and conducting stripes are covered with a 700 nm silicon oxide layer for protection. The sample is placed in the heated area in case of small samples or spread over the whole sensor using spin coating in case of thin films.

Only the small heated area, which can be considered as point heat source, is of interest. Both sensors are placed adjacent in a thermostat at temperature T_B. Measurements are either done at a single frequency changing the temperature continuously (temperature scans) or at different frequencies keeping the temperature constant (frequency scans). In the latter case temperature can be changed stepwise. To get an almost uniform temperature distribution and small errors in temperature the heating rate is limited to 5 K min^{-1}. The calorimeter can be operated in air or an inert gas as nitrogen or helium at ambient or reduced pressure.

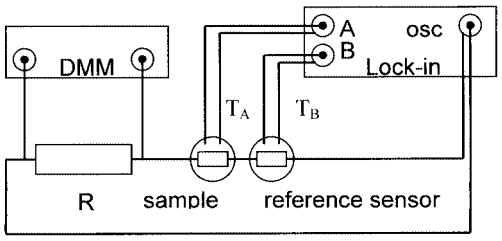

Fig.2 Schematic picture of the electric setup. Using the internal generator of the lock-in amplifier results in better phase stability. The differential signal A-B of the thermopiles is analyzed and further processed. The voltage over the known resistor R is measured with a digital multimeter to calculate heater power. All components are controlled by a computer.

The electrical scheme of the device is given in **Fig.2**. The heaters on the chips are driven by an alternating current at frequency $\omega/2$ from the oscillator of the lock-in amplifier. This results in an oscillating power at frequency ω. Amplitude and phase of the resulting oscillating temperature at frequency ω is measured with the surrounding thermopile using a digital lock-in amplifier (Model 7625 from Signal Recovery). The oscillator voltage is applied to the two sensors and a known constant resistor in series. The applied power is calculated from the voltage over the known resistor measured with a digital multimeter (PREMA 6001) or with an extra ADC input of the lock-in amplifier taking the oscillator voltage and the internal resistance of the oscillator into account.

Depending on the surrounding gas and sample thickness the available frequency range is between 1 Hz and 1 kHz. The heater power per sensor is about 10 ~50 µW, which results in a temperature oscillation amplitude and a temperature bias of less than 1 K. The frequency of maximal sensitivity depends on thermal conductivity and heat capacity of the surrounding gas. For nitrogen at ambient pressure maximal sensitivity is observed between 10 Hz and 100 Hz. For lower frequencies the losses through the gas dominate. For higher frequencies the distance between the thermopile and the heater is too large. Reducing the losses by lowering pressure the frequency range can be extended to lower values. The frequency dependence of the thermopile

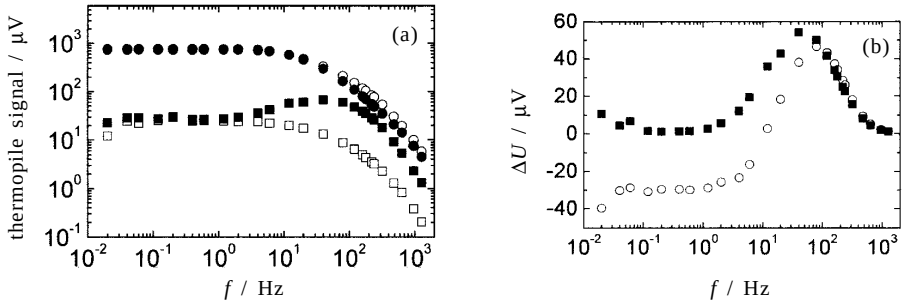

Fig.3 Frequency dependence of the thermopile signal in air at 300 K and ambient pressure. (a) shows the real part for the single sensor empty (○) and with sample (●) and two sensors in differential setup, both empty (□) and one with sample (■). In (b) the difference of empty measurement and sample measurement is shown for a single sensor (○) and for the differential setup (■).

signal for the empty and the loaded system is shown in **Fig.3(a)** and **3(b)**. The sensors were not selected according with symmetry and no other measure was applied to make the system more symmetric. The measurements were done at 300 K at ambient pressure. Due to the asymmetry of the losses a differential signal of about 25 μV is seen at low frequencies for the two empty sensors. This signal is about $1^1/_2$ order of magnitude smaller than the signal for the single sensors. In Figure 3b the difference of the empty and the loaded system is shown. The reason for the negative values for the difference of the single sensors is not yet clear. A possible explanation is a difference in the ambient conditions between the successive measurements. In the differential setup such differences are dramatically reduced. Only at very low frequencies, when the measured signal is only due to different losses through the surrounding gas, a non zero difference is measured.

Using sensors with minimal asymmetry an increase in the sensitivity by a factor 100 or above should be possible with this measurement setup. Furthermore ambient disturbances are reduced by the differential setup. This leads to a very sensitive calorimetric method able to measure in the pJ K^{-1} range and samples of one nanogram and below. The sensitivity of the calorimeter will allow to measure thin films with film thicknesses in the order of 1 nm.

Results and Discussion

The capabilities of the calorimeter are demonstrated on two examples. At first a medium sized sample of the semi crystalline polymer poly-ε-caprolactone is measured. All correction discussed above are taken into account. These are the empty measurement, the thermopile sensitivity and the terms $\cosh(\alpha_0)$ and $G/i\omega$. Because the sample mass is actually not accessible by an independent measurement the heat capacity is corrected by a factor according to the specific heat capacity of the liquid PCL at 70℃, which is available from the ATHAS databank.[29] With this factor the sample mass can be estimated as 200 ng resulting in a volume of the sample droplet of about 200×10^{-9} cm^3 which is in agreement to the microscopic observations. In **Fig.4** a temperature scan on heating and cooling with 1 K min^{-1} at 80 Hz is shown. The temperature amplitude is about 0.4 K. The supplied power was less than 40 μW to each heater.

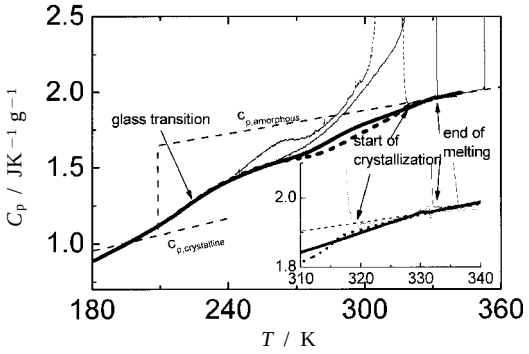

Fig.4 Temperature scans of semi crystalline poly-ε-caprolactone at 1 K min^{-1} cooling (solid line) and at heating (dotted line) Bold lines from differential AC-chip calorimeter at frequency 80 Hz and temperature amplitude ≈ 0.4 K. Thin lines from DSC scan measurements (DSC 822, Mettler Toledo). The straight dashed lines are the heat capacity for amorphous and crystalline sample from the ATHAS database.[29]

The measured heat capacity shows the expected behavior with a glass transition at about 220 K and a melting/crystallization at higher temperatures. Nevertheless a deviation from the ATHAS database curves is seen which can not be adjusted by a constant factor. A possible explanation is a change in the thermal contact of the sample which can not be measured in this setup. This could be due to the medium sized sample which has a different thermal expansion coefficient than the membrane. Using smaller samples or thin films this effect should be avoided. In **Fig.4** at cooling and at heating no pronounced peak is seen in the heat capacity from the AC-chip calorimeter at 80 Hz. The measured heat capacity is close to base-line heat capacity[30] as expected for high frequency measurements.[31] The inset in **Fig.4** shows the changes in heat capacity at the beginning of crystallization and at the end of melting in more detail. At cooling an abrupt change in the slope is seen below 320 K when the sample is crystallizing. At heating heat capacity approaches very smoothly the ATHAS data bank value around 330 K with a tiny peak at the end of melting.

Next, a polystyrene film of 15 nm thickness is measured in a broad frequency range. The polystyrene film is produced by spin coating. The thickness is measured by capacitance measurements on a sample

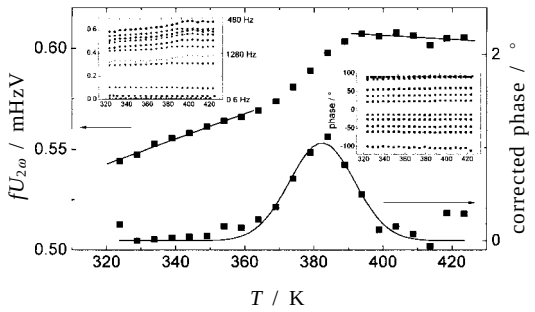

Fig.5 Signal amplitude times frequency for a polystyrene film of 15 nm thickness for a frequency of 80 Hz. The measurements are done at isotherm frequency sweeps every 5 K from 323 to 423 K. In the phase a peak in the glass transition range is seen as expected. In the inserts signal amplitude times frequency and phase for all measured frequencies are shown.

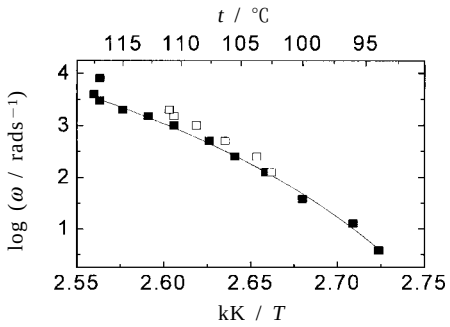

Fig.6 Arrhenius plot for the glass transition of the polystyrene film of 15 nm thickness shown in Fig.5. The solid symbols are from the half step height of the real part and the open symbols from the peak in the phase. The curve is a WLF fit to the data obtained from the real part with the parameter log (ω/rads^{-1})=8, B=250, T_0=333 K.

prepared under the same conditions.[32] Frequency sweeps from 0.6 Hz to 1280 Hz are performed and the temperature is changed stepwise from 323 K for 5 K until 423 K. The results are shown in **Fig.5**. In this case we do not correct the signal to get heat capacity. Nevertheless the glass transition temperature and relative changes of the signal are accessible. Using the real part of the measured thermopile signal the frequency dependent glass transition temperature is observed using the temperature at the half height of the step. Also in the phase a peak at the glass transition is found as common for complex heat capacity. There is an underlying step in the phase which is proportional to the real part. The phase signal is corrected subtracting this contribution as described in.[33] The maximum positions are shown in the Arrhenius plot in **Fig.6**. The data can be fitted by a WLF equation[34] as usual.

$$\log\omega = \log\Omega - \frac{B}{T - T_0} \qquad (8)$$

The Arrhenius plot shows the actual frequency range. Uncertainties in glass transition temperature determination become larger at highest and lowest frequencies because the signal decreases significantly, see upper left inset in **Fig.5**. The dominating contribution from the heat loss through the gas is demonstrated by the small values of fU for low frequencies. The step at the glass transition can be evaluated in the frequency range from 0.6 to 1280 Hz. The peak in the phase is detectable and can be used to determine the glass transition temperature in the range 20 to 320 Hz.

The probed sample mass of such a film, which is frequency dependent, one can estimate to 1 ng for an assumed effective heated area of 0.2×0.2 mm^2 at the lowest frequencies. With the heat capacity of polymers of about 1 J K^{-1} g^{-1} a sample heat capacity of 1 nJ K^{-1} is measured. From this approximation and the scatter in **Fig.5** the sensitivity of the setup can be estimated as *ca*. 50 pJ K^{-1}.

Conclusions

We describe a high sensitive differential AC-chip calorimeter based on a commercially available sensor. It is possible to measure heat capacity of medium sized samples, *ca*. 100 ng, over a broad temperature range. The high sensitivity of the differential system was demonstrated by the measurement of a 15 nm polymeric film. The effectively heated mass of such a film is about 1 ng. It is pointed out that a sensitivity of 50 pJ K^{-1} is feasible with this setup, which is sufficient to measure polymeric samples of 1 nm thickness.

The AC-chip calorimeter allows measurements over a wide frequency range up to kHz. The glass transition temperature of the 15 nm polystyrene film was determined in the frequency range 0.6 Hz to 1280 Hz. Sensitivity and frequency range could be further improved using a

sensor with even smaller heated area and closer distance between the thermometer and the heater.

Acknowledgements

The authors thank Dr. M. Wübbenhorst for providing the spin coated polystyrene samples. The work was financially supported by the German Science Foundation (DFG) Grants Schi 331/7 and 436 RUS 17/49/03.

References

1) G. Privalov, V. Kavina, E. Freire, and P. L. Privalov, *Anal. Biochem.* **232**, 79 (1995).
2) S. Wang, K. Tozaki, H. Hayashi, S. Hosaka, and H. Inaba, *Thermochim. Acta* **408**, 31 (2003).
3) H. Yao, K. Ema, H. Fukada, K. Takahashi, and I. Hatta, *Rev. Sci. Instrum.* **74**, 4164 (2003).
4) O. M. Corbino, *Physik. Zeitschr.* **XI**, 413 (1910).
5) Y. A. Kraftmakher, *Zurnal prikladnoj mechaniki i techniyeceskoj fiziki* **5**, 176 (1962).
6) P. Sullivan and G. Seidel, *Ann. Acad. Sci. Fennicae* **A VI**, 58 (1966).
7) Y. Kraftmakher, *Physics Reports* **356**, 1 (2002).
8) G. S. Dixon, S. G. Black, C. T. Butler, and A. K. Jain, *Anal. Biochem.* **121**, 55 (1982).
9) D. W. Denlinger, E. N. Abarra, K. Allen, P. W. Rooney, M. T. Messer, S. K. Watson, and F. Hellman, *Rev. Sci. Instrum.* **65**, 946 (1994).
10) S. L. Lai, G. Ramanath, L. H. Allen, P. Infante, and Z. Ma, *Appl. Phys. Lett.* **67**, 1229 (1995).
11) Technical data available at: http://www.xensor.nl/.
12) J. Lerchner, G. Wolf, C. Auguet, and V. Torra, *Thermochim. Acta* **382**, 65 (2002).
13) M. Y. Efremov, E. A. Olson, M. Zhang, Z. Zhang, and L. H. Allen, *Phys. Rev. Lett.* **91**, 85703-1 (2003).
14) L. H. Allen, G. Ramanath, S. L. Lai, Z. Ma, S. Lee, D. D. J. Allman, and K. P. Fuchs, *Appl. Phys. Lett.* **64**, 417 (1994).
15) B. L. Zink, B. Revaz, R. Sappey, and F. Hellman, *Rev. Sci. Instrum.* **73**, 1841 (2002).
16) E. A. Olson, M. Yu. Efremov, M. Zhang, Z. Zhang, and L. H. Allen, *J. Microelectromech. Syst.* **12**, 355 (2003).
17) M. Y. Efremov, E. A. Olson, M. Zhang, F. Schiettekatte, Z. Zhang, and L. H. Allen, *Rev. Sci. Instrum.* **75**, 179 (2004).
18) S. A. Adamovsky, A. A. Minakov, and C. Schick, *Thermochim. Acta* **403**, 55 (2003).
19) S. Adamovsky and C. Schick, *Thermochim. Acta* **415**, 1 (2004).
20) A. A. Minakov, S. A. Adamovsky, and C. Schick, *Thermochim. Acta submitted*.
21) M. Merzlyakov, *Thermochim. Acta submitted.*
22) A. A. Minakov, D. A. Mordvintsev, and C. Schick, *Polymer* **45**, 3755 (2004).
23) A. A. Minakov, D. A. Mordvintsev, and C. Schick, *Farad. Discus.* **128**, 261 (2005).
24) A. A. Minakov, D. A. Mordvintsev, R. Tol, and C. Schick, *Thermochim. Acta submitted.*
25) H. Huth, M. Beiner, S. Weyer, M. Merzlyakov, C. Schick, and E. Donth, *Thermochim. Acta* **377**, 113 (2001).
26) A. A. Minakov,S. B. Roy, Y. V. Bugoslavsky, and L. F. Cohen, *Rev. Sci. Instr.* (2005) accepted for publication.
27) M. Merzlyakov, *Thermochim. Acta* **403**, 65 (2003).
28) A. A. Minakov, Yu. V. Bugoslavsky, and C. Schick, *Thermochim. Acta* **317**, 117 (1998).
29) B. Wunderlich, *Pure Appl. Chem.* **67**, 1019 (1995); and http://web.utk.edu/~athas/.
30) V. B. F. Mathot, Calorimetry and Thermal Analysis of Polymers, Hanser Publishers, München (1994).
31) M. Merzlyakov, A. Wurm, M. Zorzut, and C. Schick, *J. Macromol. Sci.-Phys.* **B38**, 1045 (1999).
32) M. Wübbenhorst, V. Lupascu, H. Huth, and C. Schick, *Thermochim. Acta submitted.*
33) S. Weyer, A. Hensel, and C. Schick, *Thermochim. Acta* **305**, 267 (1997).
34) M. L. Williams, R. F. Landel, and D. J. Ferry, *J. Am. Ceram. Soc.* **77**, 3701 (1955).

Heiko Huth
University of Rostock, Institute of Physics, Universitätsplatz 3, 18051 Rostock, Germany

Alexander Minakov
A. M. Prokhorov General Physics Institute, Vavilov 38, 119991 Moscow, Russia

Christoph Schick
University of Rostock, Institute of Physics, Universitätsplatz 3, 18051 Rostock, Germany
e-mail: christoph.schick@uni-rostock.de